

Figure 1. MAS-NMR spectra of solid $\text{Li}^+(\text{en})_2\cdot\text{Na}^-$ ($t \approx -70^\circ\text{C}$): (A) ^7Li NMR spectrum; (B) ^{23}Na NMR spectrum. Chemical shifts are relative to the aqueous cations at infinite dilution.

procedure that gave pure stoichiometric samples, stable to decomposition during preparation, is described here. Although less rigorous methods can also be used, especially to prepare solutions, they can lead to some decomposition.

Weighed equimolar amounts of sodium and lithium (typically 3–5 mmol of each) were introduced into one arm of an evacuable H-cell⁹ in a helium-filled glovebox. Stoichiometric amounts of anhydrous ethylenediamine were contained in a break-seal tube that had been previously attached with Teflon heat-shrinkable tubing to a distillation sidearm on the other side of the H-cell. After evacuation to $<10^{-5}$ Torr, anhydrous ammonia was condensed on the metals to form a solution and then evaporated to leave a metal film in the H-cell. About 20 mL of anhydrous methylamine was condensed onto the metal film at -78°C , forming a dark blue solution that was poured through the glass frit into the other arm of the H-cell. This solution was frozen in a liquid nitrogen bath, the break-seal was broken, and the ethylenediamine was distilled into the H-cell, followed by a seal-off of the sidearm. A homogeneous solution formed upon standing at -30°C . All of the methylamine was then removed by distillation, leaving a gold-colored shiny film. In initial experiments designed to check the stoichiometry, the film was repeatedly washed with *n*-pentane to remove any excess ethylenediamine. In later preparations, this step was eliminated by careful control of the initial amounts of lithium, sodium, and ethylenediamine. About 20 mL of anhydrous ethylamine was then condensed onto the film, forming a deep blue, apparently homogeneous solution. Condensation of 10–15 mL of *n*-pentane, followed by standing for 12–20 h at -78°C and slow removal of the solvents by distillation at temperatures below -50°C , resulted in the formation of a gold-bronze powder. To remove traces of solvent, the H-cell was evacuated to $\sim 10^{-6}$ Torr for 12–24 h with the cell temperature kept at -35 to -78°C . The powder was transferred while cold to a storage vessel in a nitrogen-filled glove bag. Recrystallization from ethylamine by addition of *n*-pentane was used to prepare samples for analysis and NMR studies. Analysis⁷ by pH titration, dc plasma emission spectroscopy, and quantitative ^1H NMR spectroscopy confirmed the stoichiometry $\text{Li}^+(\text{en})_2\cdot\text{Na}^-$. Initial experiments showed that it is important to keep the solutions below

-50°C during solvent evaporation to avoid loss of ethylenediamine.

The polycrystalline compound melts at -23°C to form a gold-colored liquid that is stable at this temperature. Upon raising the temperature to $\sim 0^\circ\text{C}$ the solution becomes dark blue and appears to contain a precipitate (probably the metals). The gold material is *not* reformed upon cooling. Raising the temperature to $\sim 30^\circ\text{C}$ causes irreversible decomposition. Differential scanning calorimetry shows an endotherm at -30 to -20°C , a second and larger endotherm at -5 to $+5^\circ\text{C}$, and an exotherm at $+30$ to $+40^\circ\text{C}$. We interpret these changes as melting, decomplexation, and decomposition, respectively.

The solid compound at low temperatures ($<-70^\circ\text{C}$) shows ^7Li and ^{23}Na MAS-NMR peaks of both Li^+ ($\delta = 0.1$ ppm, $\Delta\nu_{1/2} = 3$ KHz) and Na^- ($\delta = -59$ ppm, $\Delta\nu_{1/2} = 720$ Hz) as shown in Figure 1. Its solution in ethylamine also shows these two peaks at $\delta = 1.8$ ppm (Li^+) and $\delta = -61$ ppm (Na^-) but with line widths of only 50 Hz. A thin solvent-free film of the material, produced by rapid evaporation of methylamine, shows the characteristic optical absorption peak of Na^- at 650 nm.

The compound is soluble to at least 0.1 M in methylamine and ethylamine at -5°C , forming gold-colored films in contact with dark blue solutions at lower temperatures. Its solubility in tetrahydrofuran, dimethyl ether, and 2-aminopropane is lower, but it was possible to prepare 0.01 M solutions in all of these solvents at -30°C . Decomplexation to metal and ethylenediamine occurs in diethyl ether. The compound is insoluble in *n*-pentane and trimethylamine. Although the powdered samples described here are polycrystalline, we have thus far been unable to grow single crystals for structure determination.

Acknowledgment. This work was supported by National Science Foundation Solid State Chemistry Grant DMR 84-14154. Some of the equipment was provided by the M.S.U. Center for Fundamental Materials Research. R.C. is grateful to the Council for International Exchange of Scholars for a Fulbright Grant for this research. We acknowledge the help of Mark Kuchenmeister, Jineun Kim, Lauren Hill, and Long Le with some of the measurements.

Pyridine Complexes of Chlorine Atoms

Ronald Breslow,*¹ Michael Brandl,¹ Jürgen Hunger,¹
Nicholas Turro,*¹ Karen Cassidy,¹
Karsten Krogh-Jespersen,*² and John D. Westbrook²

Department of Chemistry, Columbia University
New York, New York 10027

Department of Chemistry
Rutgers, The State University of New Jersey
New Brunswick, New Jersey 08903

Received July 9, 1987

The use of pyridine ester templates to direct selective steroid chlorinations has been described.³ The results indicate that a chlorine atom coordinates to the pyridine nitrogen and is then relayed to a geometrically accessible substrate hydrogen. Although many studies have been reported on chlorine atom complexes to benzene and its derivatives,^{4–7} pyridine raises some unique questions. Is the chlorine σ bonded to N or π bonded? Is it a

(1) Columbia University.

(2) Rutgers University.

(3) Breslow, R.; Brandl, M.; Hunger, J.; Adams, A. D. *J. Am. Chem. Soc.* **1987**, *109*, 3799–3801.

(4) Russell, G. A. *J. Am. Chem. Soc.* **1957**, *79*, 2977–2978. Russell, G. A. *J. Am. Chem. Soc.* **1958**, *80*, 4987–4996. Walling, C.; Mayahi, M. F. *J. Am. Chem. Soc.* **1958**, *81*, 1485–1489.

(5) Skell, P. S.; Baxter, H. N., III; Taylor, C. K. *J. Am. Chem. Soc.* **1983**, *105*, 120–121. Skell, P. S.; Baxter, H. N., III; Tanko, J. M.; Chebolu, V. *J. Am. Chem. Soc.* **1986**, *108*, 6300–6311.

(6) Bunce, N. J.; Ingold, K. U.; Landers, J. P.; Luszyk, J.; Scaiano, J. C. *J. Am. Chem. Soc.* **1985**, *107*, 5464–5472. Bunce, N. J.; Joy, R. B.; Landers, J. P.; Nakai, J. S. *J. Org. Chem.* **1987**, *52*, 1155–1156.

(7) Bühler, R. E.; Ebert, M. *Nature (London)* **1967**, *214*, 1220–1221. Bühler, R. E. *Helv. Chim. Acta* **1968**, *51*, 1558–1571.

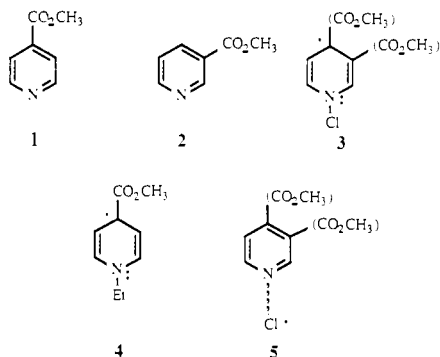
(9) Dye, J. L. *Prog. Inorg. Chem.* **1984**, *32*, 327–441.

full or loose bond? What are the kinetic and selectivity properties of these complexes?

We have addressed these questions by three techniques: classic chlorination selectivity studies,⁴⁻⁶ nanosecond laser spectroscopy and kinetics,⁶ and molecular orbital calculations. All three approaches point to similar conclusions.

Photochemically initiated free radical chain chlorination (Cl_2) of 2,3-dimethylbutane (DMB) is reported⁵ to show a selectivity ($k_{\text{tertiary}}/k_{\text{primary}}$) of ca. 50/1 at 4 M benzene in CCl_3F and low DMB concentrations, a result we have confirmed in CCl_4 solution. With pyridine instead we find that the selectivity becomes 200/1 ($\pm 20\%$) at 4 M pyridine and DMB concentrations below 0.1 M. As Skell reported for benzene,⁵ our selectivity climbs to a plateau as the DMB concentration is lowered, but no plateau is found on increasing the pyridine concentration; selectivities at a low DMB concentration (vs pyridine concentration) are 95 (2 M), 46 (1 M), 28 (0.5 M), and 18 (0.25 M). This indicates that at a DMB concentration below 0.1 M the $\text{Cl}\cdot$ equilibrates with its pyridine complex before attacking DMB but that attack on DMB involves both the complex (high selectivity) and the free $\text{Cl}\cdot$ in equilibrium (low selectivity).

With methyl isonicotinate (**1**) at 4 M the selectivity is decreased to 140/1, while with methyl nicotinate (**2**) at 4 M the selectivity is slightly less at 120/1. In these cases as well the plateau occurred



on lowering the DMB concentration but not on raising the pyridine derivative concentration. Thus all three compounds produce more selectivity than does benzene and presumably bind $\text{Cl}\cdot$ more strongly. However, the finding that the pyridine esters show less selectivity than does pyridine itself is not consistent with a fully formed σ -bond in the complexes. The ester groups should strongly stabilize the resulting π^* -type radicals **3** by conjugation³ and increase the binding constant for $\text{Cl}\cdot$. If instead the complex involves weak electron donation by the pyridine to the chlorine atom, the decreased basicity of the pyridine esters could explain our findings.

Solutions of Cl_2 in CCl_4 with aromatic complexers were irradiated with a Quanta Ray (6 ns FWHM, 3.5 mJ, 355 nm) Nd-YAG laser. Spectra were obtained with a Parc OMA III optical multichannel analyzer calibrated with a mercury lamp. With use of benzene we observed the reported chlorine atom complex^{6,7} with λ_{max} 490 nm, while with pyridine the complex had λ_{max} 334 nm. A Stern-Volmer plot of the intensity of the complex at 370 nm as a function of DMB concentration gave a rate constant⁸ for formation of the pyridine complex of $1.5 \times 10^{10} \text{ M}^{-1} \text{ s}^{-1}$ (reported⁶ for benzene $0.6 \times 10^{10} \text{ M}^{-1} \text{ s}^{-1}$). The formed complexes also decayed by second-order reactions with DMB. Benzene (0.25 M) showed a second-order rate constant⁸ of $4.4 \times 10^7 \text{ M}^{-1} \text{ s}^{-1}$, while pyridine (0.25 M) showed $2.6 \times 10^5 \text{ M}^{-1} \text{ s}^{-1}$. At these aromatic concentrations the decay involves chiefly reversible dissociation of the complex to free $\text{Cl}\cdot$, which is scavenged by DMB. Thus the pyridine/ $\text{Cl}\cdot$ association constant is ca. $34\,000 \text{ M}^{-1}$, 170 times

the reported value^{6,9} of 200 M^{-1} for benzene.

The same pyridine/benzene rate constant⁸ ratio of ca. 170–200 was observed with use of cyclohexane as a $\text{Cl}\cdot$ scavenger, as expected if this is the ratio of dissociation constants for the complexes. At a higher (5 M) pyridine concentration the second-order rate constant for reaction with cyclohexane decreased to $3.7 \times 10^4 \text{ M}^{-1} \text{ s}^{-1}$ as reaction of the undissociated complex came to predominate. With use of cyclohexane and low concentrations of pyridine derivatives, we found that the second-order decay rate of the $\text{Cl}\cdot$ adduct with methyl isonicotinate (**1**) was equal to that of the pyridine complex, within experimental error (20%), while the complex with methyl nicotinate (**2**) reacted two times faster. The similarity of binding constants for $\text{Cl}\cdot$ by pyridine, **1**, and **2** determined by this technique would again not be expected for a fully bonded adduct **3**, in which the ester groups should contribute conjugative stabilization.

Spectroscopic maxima were determined for the $\text{Cl}\cdot$ adducts to a variety of pyridine compounds. The pyridine complex λ_{max} at 334 nm shifts to ca. 350 nm for the complexes of **1** and **2**, but no long wavelength band is seen. Kosower had reported¹⁰ bands at 304, 395, and 632 nm for **4**, which can be thought of as an ethyl analogue of a fully bonded adduct **3** of $\text{Cl}\cdot$ to the nitrogen of **1**. This difference in spectra also indicates that we are not dealing with full σ bonding of $\text{Cl}\cdot$, as in **3**. With 2,6-di-*tert*-butylpyridine the $\text{Cl}\cdot$ adduct shows two absorption maxima, at 325 nm and 420 nm. This shifted benzene/ $\text{Cl}\cdot$ type spectrum is as expected if the *tert*-butyl groups block binding at nitrogen. In DMB chlorination, this pyridine derivative produces even less selectivity than does benzene.

Ab initio molecular orbital calculations including geometry optimization, with split valence basis sets augmented by d-functions on N and Cl,¹¹ predict a planar equilibrium structure (C_{2v}) for the pyridine/ $\text{Cl}\cdot$ adduct **5**. At the UHF level of theory, the Cl atom is located 2.80 Å from the N atom along the C_2 symmetry axis; the pyridine ring shows only minor distortions from the geometry calculated for free pyridine.¹² Additional calculations including correlation energy corrections, at the second-order Møller-Plesset level, shorten the equilibrium N-Cl distance considerably to 2.27 Å. This is still about 135% of a normal N-Cl bond length and one third of the way to the van der Waals contact distance. The N-Cl bonding (binding energy = 5.1 kcal/mol) is of the $3e-2\sigma$ orbital type with occupancy $(\sigma)^2(\sigma^*)^1$ (a^2A_1 ground state), in which the σ and σ^* orbitals are predominantly composed of the N lone pair and the Cl $3p_\sigma$ orbitals, respectively.¹³ The pyridine π -system still contains six electrons.

Semiempirical INDO/S ROHF-Cl calculations¹⁴ at the average (N-Cl = 2.54 Å) optimized geometry predict the appearance of

(9) An alternative value is suggested in ref 7, but it seems less well founded.

(10) Kosower, E. M.; Poziomek, E. J. *J. Am. Chem. Soc.* **1964**, *86*, 5515–5523. Hermolin, J.; Levin, M.; Kosower, E. M. *J. Am. Chem. Soc.* **1981**, *103*, 4808–4813.

(11) The ab initio calculations were carried out with the GAUSSIAN 82 (Binkley, J. S.; Frisch, M.; Raghavachari, K.; DeFrees, D. J.; Schlegel, H. B.; Whiteside, R. A.; Fluder, E.; Seeger, R.; Pople, J. A. GAUSSIAN 82, Release H, Carnegie-Mellon University, Pittsburgh, PA, 1984), and GAMESS (Dupuis, M.; King, H. F. *Int. J. Quant. Chem.* **1977**, *11*, 613–625; *J. Chem. Phys.* **1978**, *68*, 3998–4004) program packages. Basis sets employed for N and Cl, C, and H were 6-31G*, 3-21G, and STO-3G, respectively. Geometry optimizations at the UHF level included all unique geometrical parameters; at the MP2 level of theory, only the N-Cl distance was varied, while the pyridine fragment remained fixed at the UHF geometry.

(12) With smaller basis sets a second, nonplanar (C_2) minimum is located about 1 kcal/mol higher in energy than the planar minimum. This structure is characterized by a slightly longer (ca. 0.1–0.2 Å) N-Cl distance, and the N-Cl axis forms an angle of 40–45° with the pyridine plane. However, this structure collapses to the planar one when the 6-31G* basis set is used on N and Cl.

(13) Clark, T. *J. Comput. Chem.* **1983**, *4*, 404–409. Clark, T. *J. Comput. Chem.* **1982**, *3*, 112–116. Clark, T. *J. Comput. Chem.* **1981**, *2*, 261–265. Baird, N. C. *J. Chem. Ed.* **1977**, *54*, 291–293.

(14) The INDO/S calculations used parameters and included configurational interaction within the ROHF formalism as described in the following: Anderson, W. P.; Edwards, W. D.; Zerner, M. C. *Inorg. Chem.* **1986**, *25*, 2728–2732. Bacon, A. D.; Zerner, M. C. *Theor. Chim. Acta.* **1979**, *53*, 21. Krogh-Jespersen, K.; Westbrook, J. D.; Potenza, J. A.; Schugar, H. J. *J. Am. Chem. Soc.*, accepted for publication. The chlorine parameters were optimized to fit the spectral properties of chlorobenzene.

(8) With a significant radical chain, $\text{Cl}\cdot$ can be recycled. This would cause an overestimate of the rate of complex formation and an underestimate of its rate of reaction. Without degassing the solutions, our data for benzene are similar to the best values in ref 6; thus we assume that with the pyridine compounds trapping by dissolved O_2 also suppresses most of the recycling problem.

an intense charge-transfer band at $\lambda = 318$ nm ($f = 0.32$) corresponding to the electronic excitation $(\sigma)^2(\sigma^*)^1 \rightarrow (\sigma)^1(\sigma^*)^2$, in good agreement with the maximum observed at 334 nm. Furthermore, exploratory calculations indicate that the hydrido¹⁵ and alkyl radical¹⁰ adducts reported previously are indeed π^* -type radicals with a fully formed N-H or N-alkyl two-electron σ bond; the weak absorption band observed at long wavelengths in, e.g., **4**, involves excitation of the π -electron system only. The electronic structures of those radicals are thus dramatically different from the σ^* -type pyridine/Cl \cdot complexes discussed here, reflecting the relative N-X bond strengths.

Both our experimental and our theoretical studies indicate that chlorine complexes with pyridine derivatives involve a long weak bond as in **5**. When this geometry brings the chlorine near a substrate hydrogen, as it does in the steroid examples reported earlier,³ this loose (probably flexible) complex can perform a direct hydrogen abstraction with excellent selectivity.

Acknowledgment. Support of this work by grants from the NSF to R.B., NSF and AFOSR to N.J.T., and the NIH to K.K.-J. is gratefully acknowledged.

(15) David, D.; Geuskens, G.; Velhasselt, A.; Jung, P.; Oth, J. F. M. *Molec. Phys.* **1966**, *11*, 257-263. Tsugi, K.; Yoshida, H.; Hayahi, K. *J. Chem. Phys.* **1966**, *45*, 2894-2897. Caplain, S.; Castellano, A.; Cateau, J.-P.; Lablache-Combiere, A. *Tetrahedron* **1971**, *27*, 3541-3553. Zeldes, H.; Livingston, R. *J. Magn. Reson.* **1977**, *26*, 103-108.

Pressure Effect of the ¹H NMR Spectra of Organic Compounds in the Presence of Lanthanide Shift Reagents. A Formally Associative Process Characterized by Volume Expansion

E. M. Schulman,^{*1a} C. K. Cheung,^{1b} A. E. Merbach,^{1c} H. Yamada,^{1d} and W. J. le Noble^{*1b}

*Institut de Chimie Minérale et Analytique
Université de Lausanne
CH-1005 Lausanne, Switzerland
Department of Chemistry, Faculty of Science
Kobe University, Kobe 657, Japan
Departments of Chemistry
The State University of New York at Stony Brook
Stony Brook, New York 11794
The State University of New York
College at Buffalo
Buffalo, New York 14222
Received March 16, 1987*

Following the successful application of hydrostatic pressure in mechanistic investigations of organic reactions² and taking a lead from the pioneering investigation of Hunt and Taube³ in complex ion chemistry, chemists have launched a vigorous effort to apply this tool to substitution reactions of coordination compounds.⁴ The main premise in these studies has been the connection of volume decreases (as derived from pressure-induced rate increases) with associative behavior and volume increases with dissociative characteristics. This assumption has been impartially discussed, especially by Swaddle.⁵ The insertion of a water molecule into the coordination sphere of hexaquo cations in water is considered

(1) (a) At Buffalo. (b) At Stony Brook. (c) At Lausanne. (d) At Kobe.
(2) For reviews, see: (a) le Noble, W. J.; Kelm, H. *Angew. Chem., Int. Ed. Engl.* **1980**, *19*, 841. (b) Isaacs, N. S. *Liquid Phase High Pressure Chemistry*; Wiley: New York, 1981. For a much more complete listing, see: Matsumoto, K.; Sera, A.; Uchida, T. *Synthesis* **1985**, 1.
(3) Hunt, H. R.; Taube, H. *J. Am. Chem. Soc.* **1958**, *80*, 2642.
(4) (a) Kelm, H. *High Pressure Chemistry*; Reidel: Dordrecht, 1978. (b) van Eldik, R. *Angew. Chem., Int. Ed. Engl.* **1986**, *25*. (c) *Inorganic High Pressure Chemistry: Kinetics and Mechanisms*; van Eldik, R., Ed.; Elsevier: Amsterdam, 1986.

(5) For example: Swaddle, T. W. *Adv. Inorg. Bioinorg. Mech.* **1983**, *2*, 95 (see p 112). Swaddle, T. W. *Inorg. Chem.* **1980**, *19*, 3203; **1983**, *22*, 2663.
(6) Tris-6,6,7,7,8,8,8-heptafluoro-2-dimethyl-3,5-octanedionatoeuropium (III).
(7) For a review of the technology, see: Ando, I.; Webb, G. A. *Magn. Reson. Chem.* **1986**, *24*, 557.

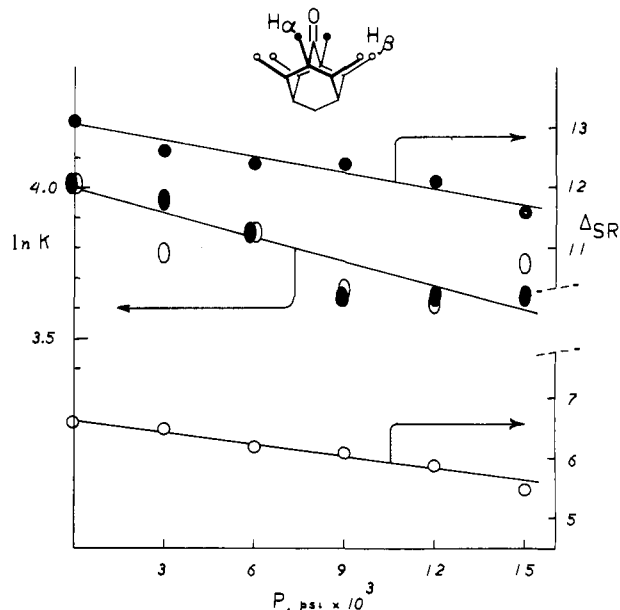


Figure 1. Pressure effects on $\ln K$ for the association of adamantanone with $\text{Eu}(\text{fod})_3$ (left vertical axis; slope related to ΔV as in the text) and on the bound shifts of H_α and H_β (right vertical axis). Solid points refer to H_α , open ones to H_β .

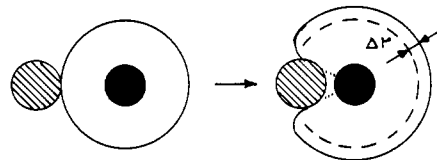


Figure 2. Schematic explanation of expansion upon association.

to be the quintessential example of a neutral molecule adding to such ions; the reaction volume is estimated to be -13 to -14 cm^3/mol .

Accordingly, we began to study pressure effects in the NMR spectra of ketone-lanthanide combinations with the hope that the increased shifts anticipated might enhance the utility of the method, perhaps even expand its applicability to new classes of compounds. Application of the assumption quoted led us to estimate that the volume decrease could be as much as 50 cm^3/mol . But this was not to be. When a solution of adamantanone and $\text{Eu}(\text{fod})_3$ in CDCl_3 is compressed at probe temperature, the well-known paramagnetic shifts of all adamantanone protons are reduced. At the same time, the slight increase in shielding of the ligand *tert*-butyl protons observed upon complexation is also reversed. This phenomenon is not an artifact of method or apparatus; it has been found with thick-walled unsupported glass capillaries in either a JEOL FX-90-Q or a Nicolet NT-300 spectrometer as well as with thin-walled capillaries inside metallic non-magnetic pressure vessels in a Bruker WP-60 instrument.⁷ The effect of 100 MPa (~ 1000 atm) pressure is roughly equal to that of dilution by a factor of 2 or more. We soon found that the result is not restricted to this complex. 5-Phenyl- and 5-*tert*-butyladamantan-2-one, piperidine, tetrahydrofuran, and cyclopentanol also exhibited pressure-reduced lanthanide-induced shifts with $\text{Eu}(\text{fod})_3$; $\text{Yb}(\text{fod})_3$ and the shielding reagent $\text{Pr}(\text{fod})_3$ showed the same effect with adamantanone. Solvent variations (CD_2Cl_2 , CCl_4) caused minor changes in the magnitude of these shifts but did not reverse any.

With the objective of learning whether these effects are due to a suppressed equilibrium population or to a reduction in the bound shift of the complex, we measured the spectra for a series